 doi:10.20944/preprints202102.0276.v1

Article

LRH-1 ameliorates hepatic triglyceride accumulation via regulation of perilipin 5 in the liver

Rubee Pantha [1], Jae-Ho Lee [1], Jae-Hoon Bae [1], Eun Hee Koh [2], Dae-Kyu Song [1] and Seung-Soon Im [1,*]

[1] Department of Physiology, Keimyung University School of Medicine, 1095 Dalgubeol-daero, Dalseo-gu, Daegu 42601, Republic of Korea.
[2] Department of Internal Medicine, University of Ulsan College of Medicine, Seoul, Republic of Korea.
* Correspondence: ssim73@kmu.ac.kr ; Tel.: +82-53-258-7423, Fax: +82-53-258-7412

Abstract: Liver receptor homolog-1 (LRH-1) has emerged as a regulator of hepatic glucose, bile acid, and mitochondrial metabolism. However, the functional mechanism underlying the effect of LRH-1 on lipid mobilization has not been addressed. This study investigated the regulatory function of LRH-1 in lipid metabolism during fasting. The wild-type (WT) and LRH-1 liver-specific knockout (LKO) mice were either fed or fasted for 24 h, and the liver and serum were isolated. During fasting, the LRH-1 LKO mice showed greater accumulation of triglycerides in the liver compared to that in WT mice. Interestingly, LRH-1 LKO liver decreased the perilipin 5 (PLIN5) expression and genes involved in β-oxidation. Additionally, the LRH-1 agonist dialauroylphosphatidylcholine also enhanced PLIN5 expression in human cultured HepG2 cells. To identify new target genes of LRH-1, these findings directed to analyze the *PLIN5* promoter sequence, which revealed −1620/−1614 to be a putative binding site for LRH-1. This was confirmed by promoter activity and chromatin immunoprecipitation assays. Moreover, fasted WT primary hepatocytes showed increased co-localization of PLIN5 in lipid droplets (LDs) compared to that in fasted LRH-1 LKO primary hepatocytes. Overall, these findings suggest that PLIN5 might be a novel target of LRH-1 to mobilize LDs and manage the cellular needs.

Keywords: liver receptor homolog-1; perilipin 5; triglyceride; fasting; lipid droplet

1. Introduction

Liver receptor homolog-1 (LRH-1/NR5A2) is a representative of the nuclear receptor 5A subfamily of orphan nuclear receptors, mainly expressed in the liver, pancreas, ovary, and intestine [1]. It is the principal regulator of glucose, bile acid, and cholesterol metabolism with varied biological roles extending from regulation of the cell cycle to the maintenance of steroid homeostasis [2,3]. In the pancreas, LRH-1 with pancreas transcription factor stimulates the expression of genes encoding pancreatic digestive enzymes and secretory proteins [4]. Moreover, LRH-1 regulates the maturation of ovarian follicles and ovulation in the ovary [5] and is responsible for mitochondrial function by regulating cytochrome p450, family 11, subfamily a, polypeptide 1 and cytochrome p450, family 11, subfamily b, polypeptide 1 in the intestinal epithelium [6]. In the liver, LRH-1 is involved in mitochondrial biogenesis and β-oxidation through the regulation of peroxisome proliferator-activated receptor gamma coactivator 1-alpha gene expression [7]. It is also involved in maintaining the pool of arachidonoyl phospholipids, which are important for normal lipid homeostasis in the liver [8]. In addition, LRH-1 liver-specific knockout (LKO) mice show endoplasmic reticulum stress-induced fatty liver, indicating that LRH-1 plays a major role in triglyceride (TG) accumulation in the liver [9].

Excess TGs in the liver are mainly reserved within lipid droplets (LDs) [10]. LDs are used to balance lipid storage and utilization and are strongly regulated in a cell type-specific manner [11]. As LDs modulate low intracellular free fatty acid levels, they play a crucial role in protecting the liver from lipotoxicity caused by excess fatty acids in nutritional stress conditions [10,12]. In addition, the mobilization of LDs reflects the metabolic state of cells and indicates changes in the LD-related proteins that contribute to the regulation of lipid metabolism and lipid homeostasis [13].

Preprints (www.preprints.org) | NOT PEER-REVIEWED | Posted: 11 February 2021 doi:10.20944/preprints202102.0276.v1

The perilipin (PLIN) protein family, which attaches to LDs, is a representative group of LD-associated proteins that utilizes the stored lipids of LDs via lipolysis [10,11]. It is composed of five members, named PLIN1–5 and is classified based on stability in a free state. PLIN1 and PLIN2 rapidly degrade in a free state; however, they exist when bound to LDs. The remaining proteins from the family, PLIN3, PLIN4, and PLIN5, are found either free in the cytosol or lining the LDs [14]. PLIN1 is found in white and brown adipose tissue (WAT and BAT), whereas PLIN2 and PLIN3 are distributed in many cell types, and PLIN2 is especially observed in hepatocytes. PLIN4 is expressed in cardiomyocytes, adipocytes, and myocytes, and PLIN5 is usually confined within tissues or cells with high oxidative capacity, namely the liver, heart, BAT, and muscle [11,14,15].

Among the PLIN family, PLIN5 has emerged as indispensable for adjusting lipid abundance. It is highly active upon fatty acid treatment in cultured cells, with a high fat diet, and upon prolonged fasting [10]. Prolonged fasting is also known to increase TG accumulation in the liver [16,17] due to increased adipose tissue lipolysis [18]. Therefore, PLIN5 is also regarded as the regulator of TG metabolism [19]. The overexpression of PLIN5 in cells enhances the expression of genes encoding proteins involved in aerobic catabolism and promotes both TG storage and fatty acid oxidation. Thus, PLIN5 rapidly mobilizes energy by sensing the nutrient demand [20].

The orphan nuclear receptor LRH-1 is activated during nutritional stress and is involved in protecting the liver from lipid overload by increasing the β-oxidation. Even though LRH-1 regulates mitochondrial biogenesis and lipid metabolism, its regulatory mechanism is not clear and the function of LRH-1 under nutritional deprivation conditions has not been completely addressed. Therefore, in this study, the regulatory function of LRH-1 was investigated during a nutrient deprivation state by utilizing wild-type (WT) and LRH-1 LKO mice in order to verifying the function of LRH-1 in cellular energy demands and lipid overloading state.

2. Materials and Methods

2.1. Animal studies

LRH-1 LKO mice were obtained by mating mice with an LRH-1 allele flanked by LoxP sites (LRH-1$^{f/f}$) with albumin-Cre transgenic mice. LRH-1$^{f/f}$ mice were Kindly gifted by Prof. Timothy F. Osborne and albumin-Cre transgenic mice were purchased from The Jackson Laboratory (Bar Harbor, Maine, USA). Eight-to-twelve-week-old WT and LRH-1 LKO male mice were used for the study. Mice were housed in a specific pathogen-free facility and fed a standard chow diet and water ad libitum. All mice were kept under 12:12-hour light-dark cycles (6 a.m.-6 p.m. light, 6 p.m.-6 a.m. dark) at 22-24 °C and 60-70% humidity. All animal experiments were performed following the guidelines provided by the Institutional Animal Care and Use Committee of Keimyung University (KM-2020-12R1).

2.2. Cell culture

HepG2 immortalized human hepatocytes and human embryonic kidney (HEK)-293T cells were cultured in Dulbecco's modified Eagle's medium (DMEM, Hyclone, Logan, UT, USA) supplemented with 10% fetal bovine serum (FBS, Hyclone) and 100 U/ml penicillin-streptomycin (P/S) as complete media. For LRH-1 agonist treatment, HepG2 cells were cultured in the presence or absence of 100 μM dialauroylphosphatidylcholine (DLPC, Sigma-Aldrich, Co., St. Louis, MO, USA) in DMEM complete media for 24 h. Primary hepatocytes were cultured in either William's Medium E (Gibco, Grand Island, NY, USA) supplemented with 10% FBS, 1% Glutamax (Gibco), and 100 U/ml P/S or DMEM media (Hyclone) supplemented with 10% FBS and 100 U/ml P/S. Cells were incubated in a humidified atmosphere containing 5% CO2 at 37 °C.

2.3. Quantitative polymerase chain reaction (qPCR)

Preprints (www.preprints.org) | NOT PEER-REVIEWED | Posted: 11 February 2021 doi:10.20944/preprints202102.0276.v1

Total RNA was isolated from the liver samples of 24 h-fasted and fed WT and LRH-1 LKO mice, as well as from HepG2 cells treated with the LRH-1 agonist DLPC, using TriZol reagent (Life Technologies, Carlsbad, CA, USA). The qPCR was performed using a CFX96™ real time system (Bio-Rad, Hercules, CA, USA) to measure the expression level of various genes (Table 1). The relative mRNA expression level was normalized to ribosomal protein L32 or ribosomal phosphoprotein P0 by calculations based on the delta-delta threshold cycle method.

Table 1. List of primers and their sequence used in qPCR.

Gene	Species	Forward primers (5′⟶3′)	Reverse primers (5′⟶3′)
L32	Mouse	ACATTTGCCCTGAATGTGGT	ATCCTCTTGCCCTGATCCTT
Lrh-1	Mouse	TCATGCTGCCCAAAGTGGAGA	TGGTTTTGGACAGTTCGCTT
Plin5	Mouse	TGTCCAGTGCTTACAACTCGG	CAGGGCACAGGTAGTCACAC
Pparα	Mouse	AGAGCCCCATCTGTCCTCTC	ACTGGTAGTCTGCAAAACCAAA
Cyp8b1	Mouse	CAAAGCCCCAGCGCCT	TTCGACTTCAAGCTGGTCGA
Cpt1-α	Mouse	CTCCGCCTGAGCCATGAAG	CACCAGTGATGATGCCATTCT
Fgf21	Mouse	CTGCTGGGGGTCTACCAAG	CTGCGCCTACCACTGTTCC
Mttp	Mouse	CTCTTGGCAGTGCTTTTTCTCT	GAGCTTGTATAGCCGCTCATT
ApoB	Mouse	TTGGCAAACTGCATAGCATCC	TCAAATTGGGACTCTCCTTTAGC
RPLP0	Human	GTGCTGATGGGCAAGAAC	AGGTCCTCCTTGGTGAAC
LRH-1	Human	CTTTGTCCCGTGTGTGGAGAT	GTCGGCCCTTACAGCTTCTA
PLIN5	Human	AGGCTGACGCAGAAGAATTG	AACAGAAGGCATTGGGCAAA

2.4. Western blot analysis

Western blot analysis was performed as described previously [21]. Briefly, protein samples were collected from the liver tissues of 24 h-fasted and fed WT and LKO mice, as well as from LRH-1 agonist-treated HepG2 cells. Anti-LRH-1 (ARP37407_P050) from Aviva System Biology (San Diego, CA 92111 USA), anti-PLIN5 (PA1-46215) from Invitrogen (Carlsbad, California, USA), anti-CPT-1α (sc-393070) from Santa Cruz Biotechnology (Dallas, Texas, USA), anti-PGC-1α (ab54481) and anti-PPARα (ab24509) from Abcam (Cambridge, MA, USA), anti-β-actin (A5441) from Sigma Aldrich (Steinheim, Germany), and anti-GAPDH (2118) from Cell Signaling Technology (Danvers, MA, USA) antibodies were purchased. Horseradish peroxidase-conjugated mouse and rabbit secondary antibodies were used for the detection of protein bands. Antigen–antibody binding was detected using a chemiluminescent detection reagent (Bio-Rad).

2.5. Plasmid DNA design and transient transfection

The promoter region of mouse *PLIN5* from −1883 to +93 was synthesized by PCR, and the band size was confirmed by running it on an agarose gel. Then, the band was extracted by gel extraction and cloned into the pGL3 basic vector, which was designated as pmPLIN5-1883/+93. In the promoter region, putative LRH-1-binding sequences were marked and deleted by site-directed mutagenesis using a Quick-change II Site-Directed Mutagenesis kit (Agilent Technologies Inc., Santa Clara, CA, USA). For transfection, HEK-293T cells were seeded on 6-well plates, and cells were transfected with pmPLIN5 with or without a murine LRH-1 and pCMV-β-galactosidase expression vector. The next day, 100 μM DLPC was administered to the cells, which were incubated for 24 h. Finally, cells were lysed in reporter lysis buffer (Promega corporation, Madison, WI 53711 USA) and luciferase assays were performed. The luciferase activity was normalized by β-galactosidase activity [22].

2.6. Lipid analysis

Preprints (www.preprints.org) | NOT PEER-REVIEWED | Posted: 11 February 2021 doi:10.20944/preprints202102.0276.v1

For lipid extraction, livers were homogenized in 2:1 (v/v) chloroform:methanol three times followed by drying under a stream of nitrogen gas. These dried samples were re-suspended in 1:1 (v/v) chloroform:methanol and 50 mM lithium chloride (LiCl) solution, and the lower layer was collected after centrifugation at 1400 *g* for 10 min. To the upper layer, chloroform was added, and the sample was re-centrifuged to collect the lower layer, which was repeated twice. Samples that were collected three times were pooled together and dried in a stream of nitrogen gas. Subsequently, dried samples were processed again and resuspended in 1:1 (v/v) chloroform:methanol maintaining the concentration of LiCl at 10 mM. After centrifugation, the lower layer was collected, and the aforementioned procedure was consecutively followed to collect the dried samples. To the dried sample, chloroform was added, and the sample was vortexed. Finally, TG and cholesterol were quantified with the TG-S and ASAN SET total-cholesterol kits (Asan pharm. Co., Gyeonggi-do, Korea) respectively, according to the manufacturer's instructions. Lipid contents were normalized to the liver tissue weight. Similarly, serum TG and cholesterol were analyzed using the TG-S and ASAN SET total-cholesterol kit. Serum non-esterified fatty acid (NEFA) levels were determined utilizing the NEFA C kit (Wako, Osaka, Japan).

2.7. Isolation and culture of primary hepatocytes

Hepatocytes were isolated from the livers of WT and LRH-1 LKO mice fed or fasted for 24 h using the perfusion method as described previously [23]. Briefly, mice were anesthetized with isoflurane (Hana Pharm. Co., Gyeonggi-Do, Korea) and laparotomy was performed to uncover the portal vein. Then, the vein was catheterized, and the liver was perfused with Earle's balanced salt solution (EBSS; WELGENE Inc., Gyeongsan, Republic of Korea) and 0.5 M EGTA to eliminate the blood, which was followed by 40 μg/ml liberase perfusion (Roche Diagnostics, Indianapolis, IN, USA) containing EBSS and 2 M $CaCl_2{\cdot}H_2O$. Next, the liver was instantly detached to a 10-cm culture dish and gently minced with 1× EBSS and 2 M $CaCl_2{\cdot}H_2O$. Next, cells were filtered through a 100-μm nylon cell strainer to remove tissue debris followed by centrifugation of the filtrate at 50 *g* for 1 min at 4 °C. Subsequently, the pellet was re-suspended in Percoll buffer (GE Healthcare, Uppsala, Sweden) and re-centrifuged at 100 *g* for 10 min at 4 °C to collect the viable hepatocytes in the pellet. Finally, the cell pellet was gently resuspended in William's Medium E (Gibco) supplemented with 10% FBS, 1% Glutamax, and 100 U/ml P/S, successively plating the cells on collagen-coated culture dishes for 3~4 h.

2.8. LD staining

To mark LDs with Oil red-O, WT and LRH-1 LKO mice were sacrificed after feeding or fasting for 24 h and livers were removed immediately. The liver samples were cut into 10-μm sections and fixed with 4% paraformaldehyde for 10 min at room temperature. Similarly, for staining lipid droplets via BODIPY (Invitrogen), primary hepatocytes isolated from WT and LRH-1 LKO mice were seeded on an 8-well chamber. Cell were grown overnight either in fed (DMEM, 10% FBS, 1% P/S) or in fasting (DMEM, 2% LPDS, 1% P/S) media. The next day, hepatocytes were fixed with 4% paraformaldehyde for 10 min at room temperature. Then, cells were treated with blocking solution (1% BSA in DPBS) for 30 min followed by overnight incubation with a PLIN5 antibody (NB110-60509, Novus Biologicals, Centennial, CO, USA) at 4 °C. The next day, cells were treated with a secondary antibody (Alexa Fluor 594, Invitrogen) and incubated for 1 h in the dark at room temperature. Subsequently, cells were stained with 2 μM BODIPY™ (493/503; Invitrogen) and incubated for 10 min at room temperature. Finally, cells were covered with mounting medium and then observed using confocal laser scanning microscopy (Leica Microsystems, Wetzlar, Germany).

2.9. Chromatin immunoprecipitation (ChIP) assay

Chromatin immunoprecipitation assays (ChIP) was performed as described previously [23]. Briefly, chromatin was prepared from liver tissue of WT and LRH-1 LKO mice

Preprints (www.preprints.org) | NOT PEER-REVIEWED | Posted: 11 February 2021 doi:10.20944/preprints202102.0276.v1

fed or fasted for 24 h. Liver tissues were minced and crosslinked with 1% paraformaldehyde and rotated for 8 min at room temperature. Crosslinking was stopped by adding 0.125 M glycine, and then, samples were rotated for an additional 5 min at room temperature. Finally, total chromatin was extracted from liver tissues and sonicated enough to obtain DNA fragments of 200–500 bp. Next, DNA were subjected to ChIP using an anti-LRH-1 antibody (sc-393369X) from Santa Cruz Biotechnology (USA), and then qPCR was performed.

2.10. Statistical analysis

Data were analyzed utilizing GraphPad Prism 8.4 software (GraphPad Software Inc., San Diego, CA, USA). Data are presented as the mean ± SEM. Statistical differences between groups were analyzed using a two-tailed student's t-test. Differences with *P*-values < 0.05 were declared significant.

3. Results

3.1. LRH-1 mitigates hepatic lipid overload

To understand the function of LRH-1 in regulating TGs in a nutrient deprivation state, WT and LRH-1 LKO mice were either fed or fasted for 24 h and the liver (Figure 1A) and serum were isolated to examine hepatic and serum TG levels. Initially, livers from LRH-1 LKO mice starved for 24 h displayed higher accumulation of lipids compared to that in livers of starved WT mice based on Oil red-O staining (Figure 1B). Furthermore, the quantification of staining also confirmed an increase in lipid levels in the LRH-1 LKO liver (Figure 1C), implying the necessity for further analysis of lipid levels in the liver and serum. Interestingly, fasted LRH-1 LKO mice exhibited remarkably escalated hepatic TG levels compared to those in fasted WT mice (Figure 1D). However, there was no significant difference between the fed mice of either genotype. In contrast, hepatic cholesterol was not altered between the genotypes in either fed or starved conditions (Figure 1E). Surprisingly, LRH-1 LKO mice either fed or starved showed a notable decrease in serum TG levels compared to those in WT mice (Figure 1F). However, serum cholesterol and NEFA levels were not altered significantly (Figure 1G,H). These findings suggest that the loss of LRH-1 results in a buildup of lipids in the liver, indicating that LRH-1 might be a key regulator in balancing the hepatic lipid content.

Preprints (www.preprints.org) | NOT PEER-REVIEWED | Posted: 11 February 2021 doi:10.20944/preprints202102.0276.v1

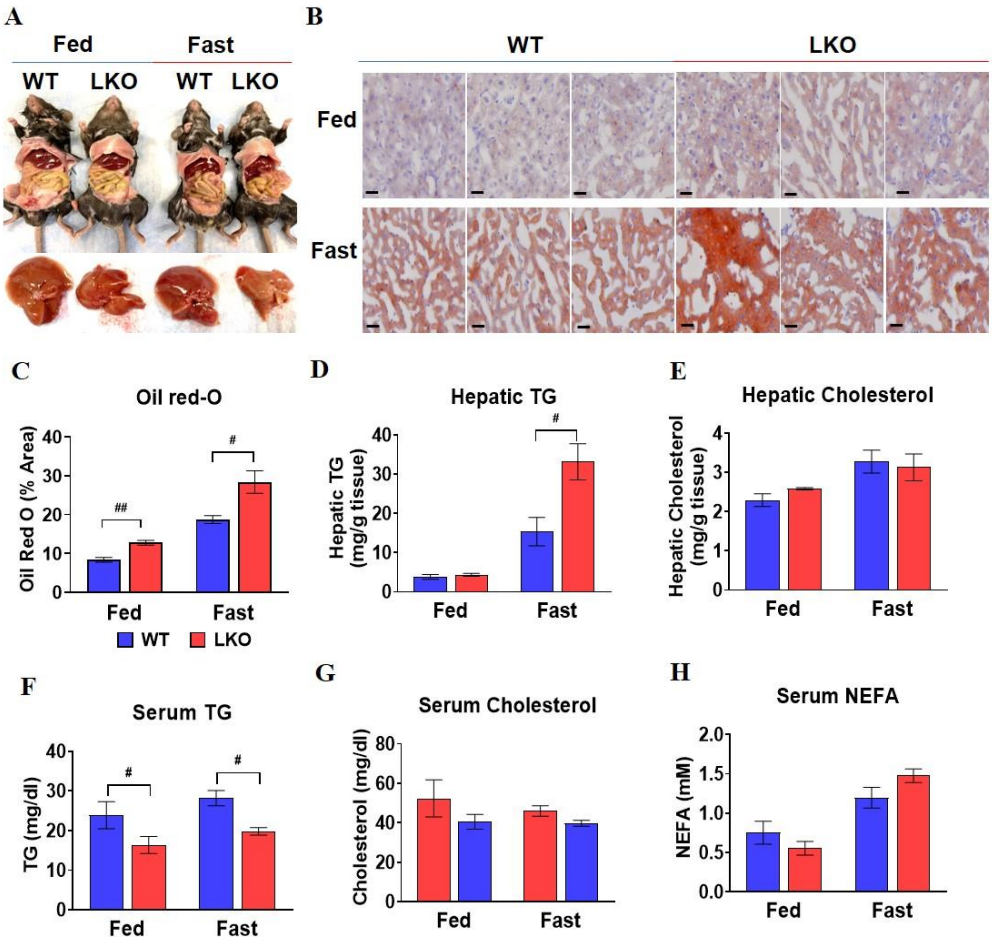

Figure 1. Lipid profile analysis in 24 h-fasted and fed mouse. (**A**) Dissection image of 24 h-fasted and fed WT and LRH-1 LKO mice along with their isolated livers. (**B**) Oil red-O staining of liver tissue (scale bar = 30 µm). (**C**) Quantification of staining in % area shown in B. (**D**), Hepatic triglycerides levels. (**E**) Hepatic cholesterol levels. (n=4/group). (**F**) Serum triglycerides levels. (**G**) Serum cholesterol levels. (**H**) Serum NEFA levels. (n=3-4/group). #$p < 0.05$, ##$p < 0.01$; WT vs LKO. WT, wild type; LKO, liver-specific knockout; TG, triglycerides; NEFA, non-esterified fatty acids.

3.2. LRH-1 induces expression of PLIN5 and fatty acid oxidation-related genes

To discover new potent target genes of LRH-1 involved in lipid metabolism, the mRNA and protein expression of various genes was examined in liver samples of either fed or starved WT and LRH-1 LKO mice. The expression levels of *Lrh-1* and its target genes were measured to confirm liver-specific LRH-1 knockout. As expected, the expression level of Lrh-1 (Figure 2A) and its target genes (Figure 2B,C) were highly reduced in LRH-1 LKO livers.

Lipid analysis suggests LRH-1 to be the key player in lipid metabolism, which functions by diminishing the TG content in the liver. In the liver, PLIN5 is known to regulate lipid metabolism [10] by promoting or inhibiting the hydrolysis of LDs [24]. Therefore, the mRNA and protein expression of PLIN5 was measured. Interestingly, as *Lrh-1* expression was augmented, the *Plin5* level was also increased in the livers of WT fasted mice. However, the expression of *Plin5* was diminished markedly in the livers of either fed or starved LRH-1 LKO mice (Figure 2D).

Preprints (www.preprints.org) | NOT PEER-REVIEWED | Posted: 11 February 2021 doi:10.20944/preprints202102.0276.v1

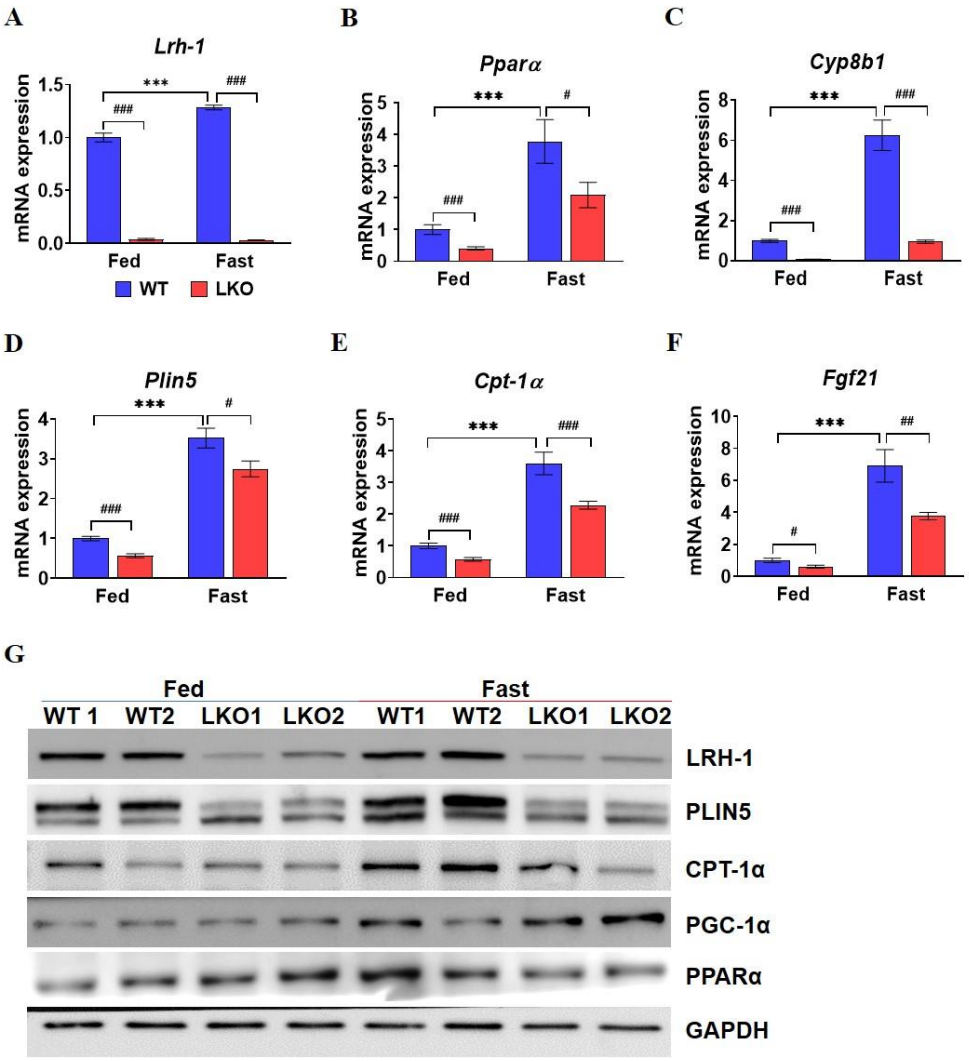

Figure 2. LRH-1 regulates perilipin 5 (PLIN5) gene and β-oxidation. All results were examined in 24 h-fasted and fed livers. (**A**) mRNA expression level of Lrh-1. (**B, C**) mRNA expression level of LRH-1 target genes. (**D**) mRNA expression levels of Plin5. (**E**) mRNA expression of fatty acid oxidation-related gene. (**F**) mRNA expression level of β-oxidation enhancer gene. (n=5/group). (**G**) Western blot for protein analysis in 24 h-fasted and fed WT and LRH-1 LKO mice. GAPDH was used as a loading control. # $p < 0.05$, ## $p < 0.01$, ### $p < 0.001$, WT vs. LKO, *** $p < 0.001$, WT fed vs. WT fast. *Cpt-1α*, carnitine palmitoyltransferase 1alpha; *Cyp8b1*, cytochrome p450 8b1; *Fgf21*, fibroblast growth factor 21; GAPDH, glyceraldehyde-3-phosphate dehydrogenase; Pparα, peroxisome proliferator-activated receptor alpha.

Additionally, TGs and β-oxidation are strongly interconnected with lipid metabolism. To understand the different liver phenotypes in WT and LRH-1 LKO mice, the expression of genes involved in fatty acid β-oxidation was measured. *Cpt1α*, a regulator of fatty acid β-oxidation [25] was expressed at remarkably lower levels in the livers of either fed or starved LRH-1 LKO mice. Nevertheless, expression was highly escalated in livers of WT fasted mice (Figure 2E). *Fgf21*, an oxidation enhancer and lipogenesis inhibitor [26] also followed a similar trend. Either fed or starved LRH-1 LKO mice showed significantly diminished *Fgf21* expression, whereas starved WT mice exhibited an increase in the expression of *Fgf21* (Figure 2F). Moreover, protein levels of LRH-1, PLIN5, CPT-1α, PGC-1α and PPARα were measured (Figure 2G). Protein levels of LRH-1 and PLIN5 were remarkably decreased in either fed or fast LRH-1 LKO mice. Also, protein levels of CPT-1α decreased in LRH-1 LKO mice. These findings suggest that PLIN5 is a putative target of LRH-1 and that the loss of LRH-1 results in a decline in β-oxidation-related genes.

Preprints (www.preprints.org) | NOT PEER-REVIEWED | Posted: 11 February 2021 doi:10.20944/preprints202102.0276.v1

3.3. An LRH-1 agonist amplifies PLIN5 gene expression

To determine whether PLIN5 is regulated by an LRH-1 agonist, human cultured HepG2 cells were treated with 100 μM DLPC for 24 h and the gene expression and protein levels of PLIN5 were measured. In the presence of DLPC, a considerable elevation in the mRNA expression of *PLIN5* was observed (Figure 3B). Moreover, DLPC treatment significantly increased PLIN5 protein levels (Figure 3C). Protein levels expressed in western blotting were quantified using computerized image analysis (ImageJ) (Figure 3D,E). These observations indicate that PLIN5 could be regulated by an exogenous agonist of LRH-1, implying that LRH-1 guides PLIN5.

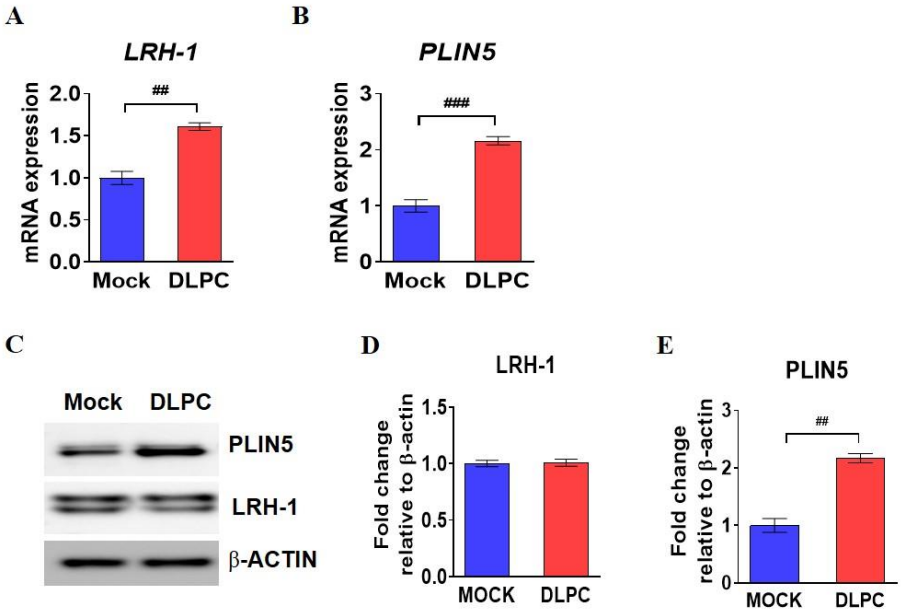

Figure 3. Enhancement of PLIN5 gene expression by LRH-1 agonist. Experiment was performed in HepG2 cells by treatment with 100 μM DLPC for 24 h. (**A**) Expression of *LRH-1* gene after treatment with DLPC. (**B**) Expression of *PLIN5* gene after treatment with DLPC. (**C**) Western blot for protein analysis of PLIN5 and LRH-1 after DLPC treatment. (**D,E**) Fold change of LRH-1 and PLIN5 proteins relative to β-actin, which was used as a loading control. These experiments were performed in triplicate. ## $p < 0.01$, ### $p < 0.001$, Mock vs. DLPC. DLPC, dialauroylphosphatidylcholine.

3.4. Putative LRH-1-binding regions in PLIN5 promoter region

In an endeavor to discover potent LRH-1-regulated genes, the LRH-1-binding regions in the *PLIN5* promoter sequence were analyzed by ChIP sequencing (ChIP-Seq) analysis using a published mouse ChIP-Seq data set for LRH-1 [27]. As expected, the ChIP-Seq analysis of *PLIN5* resulted in the identification of LRH-1-binding peaks in the promoter region (Figure 4A). Furthermore, *PLIN5* proximal promoter sequences were mapped utilizing the UCSC genome browser to identify the LRH-1-binding sites. The *PLIN5* promoter region was found to have four putative LRH-1-binding regions with direct orientations (−112/−106, −719/−713, −976/−970, and −1620/−1614 from the transcription starting site; Figure 4B). These data suggest that PLIN5 might be a direct target of LRH-1.

3.5. PLIN5 promoter activity is stimulated by LRH-1

To confirm whether LRH-1 controls *PLIN5* at a transcriptional level by binding its promoter, the *PLIN5* promoter region was cloned upstream of the luciferase expression reporter gene (Figure 5A). The *PLIN5* promoter construct was co-transfected with or without the LRH-1 expression plasmid and cells were treated with 100 μM DLPC. The *PLIN5* promoter activity increased significantly in the presence of the LRH-1 expression vector and DLPC (Figure 5B). In addition, to distinguish the main LRH-1-binding sites among the four putative sites in the *PLIN5* promoter, each putative LRH-1-binding site was

Preprints (www.preprints.org) | NOT PEER-REVIEWED | Posted: 11 February 2021 doi:10.20944/preprints202102.0276.v1

deleted from the construct. The deletion at the putative site −1620/−1614 diminished luciferase activity in response to LRH-1 in comparison to that with the other sites (Figure 5C).

This finding shows that −1620/−1614 in the *PLIN5* promoter region was the conserved site for LRH-1 binding and its removal in the construct diminished the response to LRH-1. Furthermore, binding of the LRH-1 at the −1620/−1614 site was verified by a ChIP assay performed on liver samples from 24 h-fasted and fed WT and LRH-1 LKO mice. When the sample was treated with the LRH-1 antibody, enrichment of the LRH-1 binding site −1620/−1614 was markedly elevated in livers of starved WT mice compared to that in fed WT mice. In contrast, enrichment in livers from LRH-1 LKO mice either fed or starved declined. Moreover, there were significant differences between the genotypes for either fed or starved mice (Figure 5D). These results suggested that the −1620/−1614 site in the *PLIN5* promoter region is responsible for the transcriptional regulation by LRH-1.

A

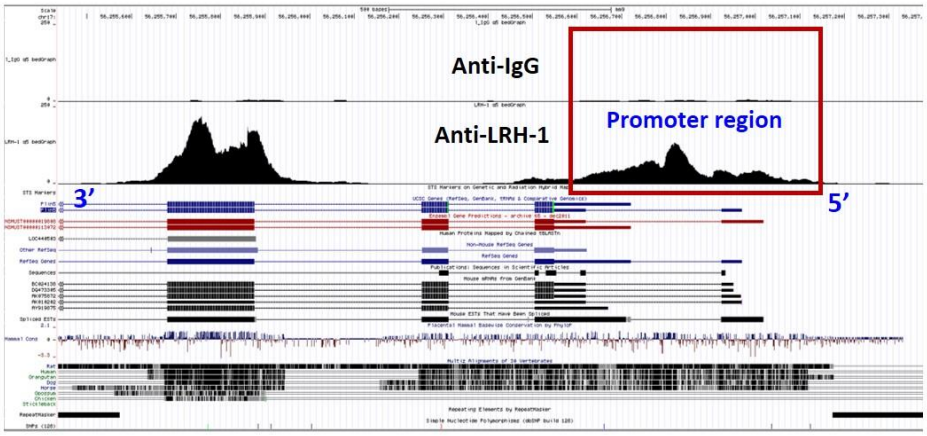

B

-1883	CCCACCCTCTGCCTTATGTTTTAAGACAGGATCTCTGGCCGGGCGGTGGTGGCGCATGCCTTTGATCCCAGCACTTGGGAGGCAGA	-1798
-1797	GGCAGGTGGATTTCTGAGTTCGAGGCCAGCCTGGTCTACAGAGTGAGTTGCAGGACAGCCAGGGCTACACAGAGAAACCCTGTCT	-1713
-1712	CGGGAAAATAAATAAATAAAAAATCTCTGACTGGCCAGCTGAGAGCCTCGGGATCTTTCTGCCTCTTTCTCTGCCTCTGCCTCCCAG	-1626
-1625	AGCTGAGGTCACACACATGAGCCAGTGTCACACATGACAAATGTGTCAAATTGAGGTCTTCCGGCTTACATGATAAGTGATAAGCA	-1540
-1539	CTTTACTGACAGTGACTGCTCTCCAGATCCTTCCCACTGTATAGCCCTGACTCTCCTGGAACTTGCTCTGTAAGCTGGCTGGTCTCAA	-1452
-1451	AGTCAGAGGTCCTCCTGCCTCTACCTCCTGAGTGCTGGGATTAAAGTCCTGCATCACAACCCAGCTTTAGTTTTTTTCACCCCCTAG	-1365
-1364	ACAGAGGGACTCTGCCCATTGAGAGGCAGGGGTGTGGATTTTTTTTTTAAAGGCCCGGTTTCATATTGCCCAGGCTGGCCTCAAATT	-1278
-1277	TGCTATAAGCCTAGGGTGATTTGAGCTCATGATTCTCCTGTCTCCACCTTGTGGCTCTGGGTGACAAGCATATGACTGGGCAAAACT	-1191
-1190	AGGCTTCTCACCCCAGTCCTGCAGAGGGAGCTGGGGAGAGTGGGTTAAAACTTGGGTCTCAGTTTGCTGATCTGTAAAATGGGGTC	-1105
-1104	AGAACTGACAGGCTTAACAGCTCTCAGGATTAAACAGCAGATTAAAAATAAGATGGAGGCCAGAGAGACCACCCATGGCTTAACA	-1020
-1019	GCTCAGGCTGGAGTTCCAGTCCCAGCATCCACATGATAGCTCAAGGTCACATGTTACTCCAGTCACAGGGGGTCTGTCAACTTTACT	-933
-932	GGCCTCTGTGGGGATCAGGCATCTGTGGATCATGACAGATGGAACATATCAACAAAACACCAGGACACATAGACGTAATAATAAT	-848
-847	AATAACAAAGGAAGTGGGCCTCAGAAGGCAGTCAGCCGAGCACCCACAGATCTGGGTTCACGCCCAGCACCACATAAACATGTGT	-763
-762	GGTGTGGCACATCTGTTGTCTTAGCCACTGGGTGGTGCGTTCAAGGTCATCCTTGGCTATGTGGTTACTTTGAGGCTATCCTGGGCT	-676
-675	ATATAGTGAGTTCTGGTCAAGTCTTGACTACAGAGAGAGAGTCTGAATCAAACAAAACAAACGGAAAAGACTGAAGAATGAGAA	-592
-591	AGTCGCCGGGCGTGGTGGCTCATGCCTTTAATCCCAGCACTTGGGAGGCAGAGGCAAGGTGGATTTCTGAGTTCGAGGCCAACCTG	-506
-505	ATCTACAAAATGAGTTCCAGGATAGCCAGAGAAAACCTGTCACAAAAAACAAAACAAAACAAAACAAAAAAAAAACAACAAAAG	-422
-421	AAGAAGGAGGAGGAGGAGGAGAAAAAAGGAGGAGGAGAAAAAAGAGGAGAAGGAGAAGGAGAAGGAGAAGGAGAAGGAGAA	-341
-340	GGAGAAGGAGAAAGAAGAAGAAAAGTCCTCAGTCGCCGGGCGGATTTCTGAGTTCGAGGCCAGCCTGTTCGGTCTACAGAGTGAG	-256
-255	TTCCAGGACAGCCAGAGCGATACAGAGAAACCCTGTCTCGAAAAAACCAACCAACCAACCAACCAAAAACCAACCAACCAACCA	-172
-171	ACCAACCAATCAAACAAACAAACAACAACAACAAAAAGAAAGTCCTCAGTCCTAGTCTGAGGTCAGCCATGGTGACTGGACCAGG	-87
-86	ATTCAGCGTCCCTGAGCCGCTATGGCAACCATGGCGCCTGTGGGGGGCGGGGAAGCTCCAGATCCACCCCCGGCGGCGCCTCATTG	-1

Figure 4. Predicted LRH-1 binding sites on mouse PLIN5 gene. (**A**) LRH-1 response elements on the mouse liver chromosome were obtained from the LRH-1 ChIP-Seq data and identified peaks that mapped to the mouse PLIN5 promoter using the UCSC Genome Browser. (**B**) PLIN5 promoter sequence from -1 to -1883 from the transcriptional start site (+1). Arrows designates putative LRH-1 binding sites. ChIP-Seq, chromatin immunoprecipitation sequencing.

Preprints (www.preprints.org) | NOT PEER-REVIEWED | Posted: 11 February 2021 doi:10.20944/preprints202102.0276.v1

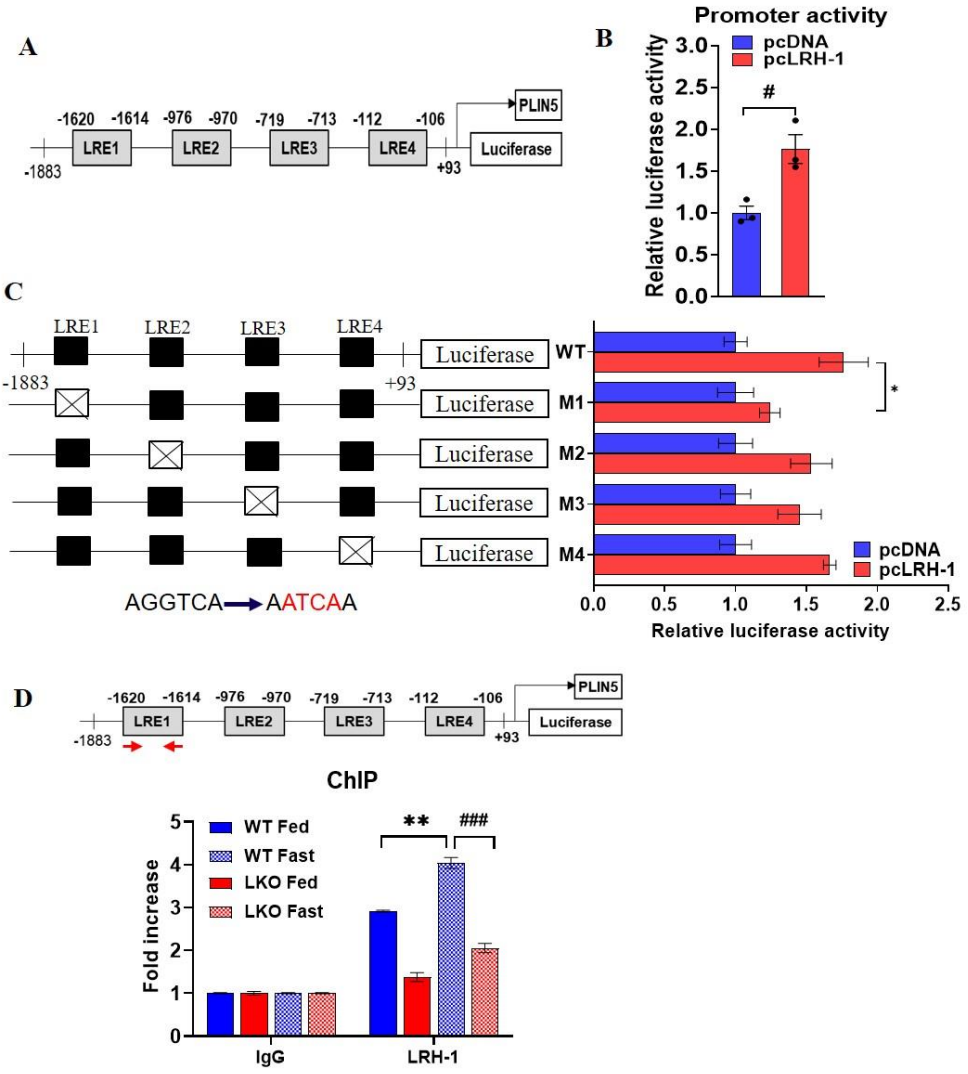

Figure 5. LRH-1 stimulates PLIN5 promoter activity by binding between the -1620 and -1614 promoter region. (**A**) Representation of putative LRH-1 binding sites in PLIN5 promoter region. (**B**) HEK-293T cells were transfected with pmPLIN5 containing the PLIN5 promoter upstream of the luciferase reporter gene along with a pcDNA or LRH-1 expression vector. (**C**) LRH-1 deletion mutants from the PLIN5 promoter region co-transfected with pcDNA or LRH-1 expression vector. The deleted sequences were shown in boxes. These experiments were performed in triplicate. (**D**) ChIP assay measured in 24 h-fasted or fed WT and LRH-1 LKO livers. (n=3/group). # $p < 0.05$, pcDNA vs pcLRH-1, ### $p < 0.001$, WT fast vs. LKO fast, * $p < 0.05$, ** $p < 0.01$, WT fed vs. WT fast. ChIP, chromatin immunoprecipitation.

3.6. LRH-1 controls PLIN5 to regulate LDs in mouse hepatocytes during nutritional stress

To evaluate the regulation of LDs via LRH-1, primary hepatocytes were isolated from WT and LRH-1 LKO mice to perform BODIPY staining. Primary hepatocytes were grown either in complete or fasting media to understand the regulatory mechanism of LRH-1 during nutrient deprivation in the liver. In the fasting media, PLIN5 surrounding the LDs was more abundant in the WT hepatocytes than in the LRH-1 LKO hepatocytes. Moreover, during fasting conditions, BODIPY was staining clearly increased in the LDs of LRH-1-null hepatocytes relative to that in WT hepatocytes. Nevertheless, the sizes of the LDs in hepatocytes were found to be distinct and increased in WT fasted mice compared to that in LRH-1 LKO mice (Figure 6A). Additionally, the co-localization of PLIN5 with LDs was quantified, which correlated with the aforementioned conclusion. The co-localization of PLIN5 in LDs was increased in WT cells with fasting media compared to that in complete media (Figure 6B).

Preprints (www.preprints.org) | NOT PEER-REVIEWED | Posted: 11 February 2021 doi:10.20944/preprints202102.0276.v1

Next, to verify alterations in the lipid quantity in the liver and serum, the mRNA expression of microsomal triglyceride transfer protein (*Mttp*), a key gene responsible for the assembly and release of lipoproteins, was measured. The LRH-1 LKO mice either fed or starved showed remarkably decreased *Mttp* mRNA expression compared to that in WT mice (Figure 6C). Furthermore, expression of the apolipoprotein B (*ApoB*) gene, a principal component present in very low-density lipoproteins (VLDLs) was measured. However, there was no significant differences between the genotypes (Figure 6C). Taken together, the loss of LRH-1 decreases PLIN5 co-localization in the LDs. Moreover, LRH-1 deficiency increases TGs in the liver by decreasing TGs secretion, leading to a surplus in the LDs.

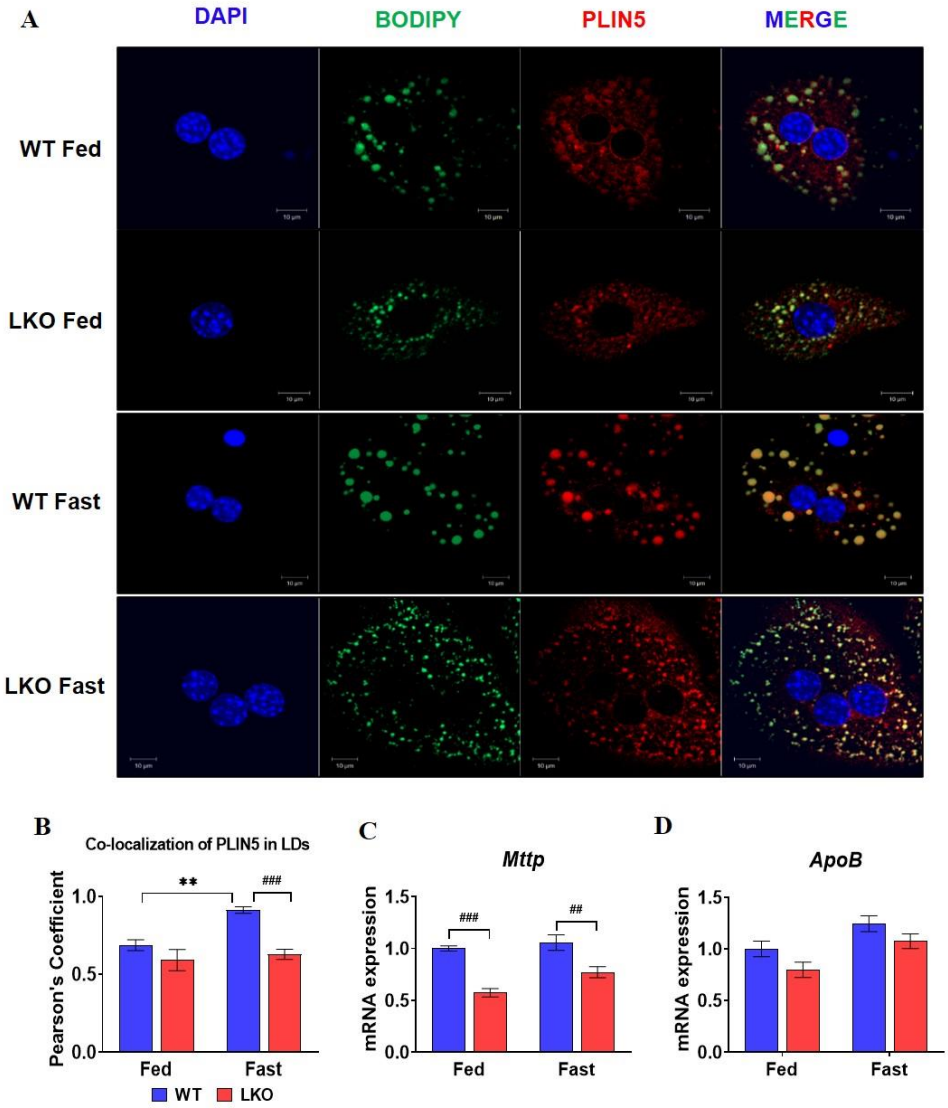

Figure 6. LRH-1 controls PLIN5 and mobilizes the lipid droplets. (**A**) BODIPY staining in primary hepatocytes grown in complete or fasting media followed by overnight incubation of PLIN5 antibody. (**B**) Co-localization of PLIN5 in LDs shown in A. (n=3/treatment group) (**C, D**) mRNA expression of genes related to VLDL secretion measured in 24 h-fasted or fed livers. (n=5/group). ## $p < 0.01$, ### $p < 0.001$, WT vs LKO, ** $p < 0.01$, WT fed vs. WT fast. *ApoB*, apolipoprotein B; LDs, lipid droplets; *Mttp*, microsomal triglyceride transfer protein; VLDL, very low-density lipoproteins.

4. Discussion

 doi:10.20944/preprints202102.0276.v1

Hepatic LRH-1 is a transcriptional regulator of glucose metabolism and bile acid homeostasis [28]. This study discovered PLIN5 as a direct target of LRH-1 and explored the function of LRH-1 in the liver during a state of nutritional deprivation. Prolonged fasting is known to result in hepatic TG accumulation due to mobilization of fatty acids from adipocytes to the liver [29]. In this study, fasting increased the accumulation of liver TGs more readily in the livers of LRH-1 LKO mice compared to that in WT livers. The elevation of hepatic TGs in the liver might be due to a decrease in β-oxidation. As expected, livers of LRH-1-null mice either fed or starved showed the markedly diminished expression of key genes responsible for β-oxidation, as well as their enhancer gene, indicating the possible accumulation of lipids in the liver. Recent studies on LRH-1 LKO mice revealed that LRH-1 promotes β-oxidation and mitochondrial biogenesis [7]. Incidentally, this result coincides with the previous findings in PLIN5-LKO mice, demonstrating elevated hepatic TG levels and a reduction in fatty acid oxidation in the liver [10]. However, these findings were in contrast with the reported research performed by Wang et al [29]. They reported decreased TGs in the liver and increased β-oxidation in the whole body PLIN5-KO mice. Together, this suggests close phenotypic similarity between LRH-1 and PLIN5 due to the transcriptional regulation of PLIN5 by LRH-1.

Interestingly, starved LRH-1-LKO mice exhibited a decrease in serum TG levels compared to that in WT mice. Altered liver and serum TG levels between the genotypes were also observed, which might be due to a decrease in TG secretion from the liver [30]. Therefore, the genes involved in VLDL secretion from the liver were measured. The gene expression of *Mttp*, a key player in VLDL secretion was markedly decreased in the livers of LRH-1-LKO mice; however, *ApoB* was unaltered. Moreover, the activation of PPARα in the liver enhances the expression of *MTTP* [31], and it was reported that PPARα also activates PLIN5 in the liver [32]. Furthermore, a decrease in TG secretion was reported in PLIN5-LKO mice [10]. Collectively, these data suggest that MTTP might be responsible for decreasing serum TGs in the livers of LRH-1 LKO mice.

Transcription factors often bind and sense lipid molecules [33]. LRH-1 binds to the −1620/−1614 binding sequence in the *PLIN5* promoter region for its transcriptional regulation, which was confirmed by promoter activity and ChIP assays. In addition, DLPC, as an agonist of LRH-1, which has a previously established role in the synthesis of bile acids and reduction of hepatic triglycerides [34], increases the mRNA expression of PLIN5. Therefore, these findings indicate that LRH-1 regulates PLIN5 at the transcriptional level.

PLIN5 balances fatty acid requirements to meet cellular needs, protecting mitochondria during extreme fatty acid flux with low-energy demands and encouraging fatty acid mobilization and oxidation with high-energy demands [35]. Based on BODIPY staining, starved WT hepatocytes demonstrated the utilization of LDs, whereas lipids were accumulated in the fasted LRH-1 LKO hepatocytes. Furthermore, PLIN5 and BODIPY staining clearly resulted in more intense red and green fluorescence, respectively, implying the co-localization of PLIN5 in LDs during starvation in WT hepatocytes. This indicates that the loss of LRH-1 decreases PLIN5 co-localization in LDs and increases the lipid content. Surprisingly, in the starved WT hepatocytes, the size of the LDs was increased and distinct compared to that in starved LRH-1 LKO hepatocytes. However, the quantity of lipids was increased in the fasted LRH-1-LKO hepatocytes. A previous study reported a decrease in the amount and size of LDs in the whole body PLIN5-KO mice [29]. However, in this study, the number of LDs increased in the LRH-1 LKO mice. PLIN5 regulates both the storage and usage of TGs and is regarded as metabolically protective [36]. In fasted WT hepatocytes, LRH-1 regulates PLIN5 to protect the liver by increasing the influx of TGs within the LDs. As a result, this increases the size of LDs. In addition, it promotes fatty acid oxidation to meet cellular energy demands during starvation, resulting in fewer LDs. In contrast, the lack of LRH-1 in the LRH-1 LKO mice attenuated PLIN5 expression, resulting in small-sized LDs and increasing their numbers. This might be the mechanism underlying the changes in the size and quantity of LDs, respectively. Overall, these observations indicate that LRH-1 regulates PLIN5 to mobilize LDs and balances hepatic lipid contents.

Preprints (www.preprints.org) | NOT PEER-REVIEWED | Posted: 11 February 2021 doi:10.20944/preprints202102.0276.v1

In summary, this study uncovered the function of LRH-1 in the liver during nutrient deprivation and presents a novel target of LRH-1 in the liver. Results further suggest the necessity of LRH-1 in lipid management to protect the liver from lipid accumulation. In the liver, LRH-1 regulates PLIN5 to mobilize lipids and maintains this balance during nutritional deprivation situations (Figure 7). Additionally, LRH-1 regulates PLIN5 to equilibrate the cellular needs and storage of lipids, thus protecting the liver from metabolic diseases associated with a fatty liver. Although LRH-1 is involved in managing the lipid content in the liver, further studies are required to assess the possible targeting of this molecule for the treatment of nonalcoholic steatohepatitis. Thus, this study might be a platform to elucidate the mechanism underlying the treatment of nonalcoholic steatohepatitis and could be beneficial for the protection of the liver.

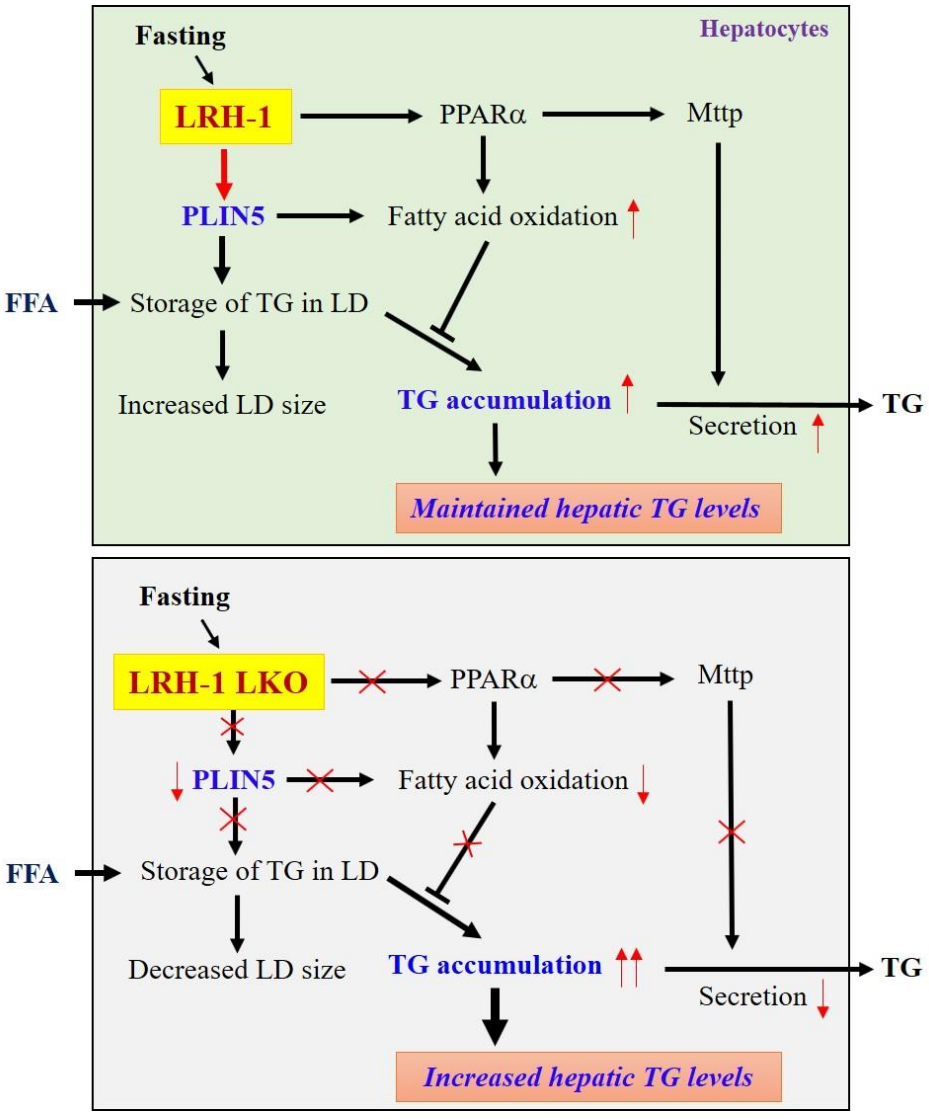

Figure 7. Scheme illustrating the role of LRH-1 in liver during nutrient deprivation state. LRH-1 regulates PLIN5 and mobilizes TGs in the liver during fasting. Deletion of LRH-1 increases the TGs in the liver during fasting by lowering the β-oxidation and TGs secretion. FFA, free fatty acids.

Author Contributions: Conceptualization, R.P. and S.S.I.; methodology, R.P. and J.H.L.; software, R.P. and J.H.L.; validation, S.S.I.; formal analysis, R.P. and J.H.L.; investigation, R.P.; resources, S.S.I.; writing—original draft preparation, R.P.; writing—review and editing, S.S.I., J.H.B., and

D.K.S.; supervision, S.S.I.; project administration, S.S.I.; funding acquisition, S.S.I. All authors have read and agreed to the published version of the manuscript.

Funding: This research was funded by grants of the Korea Research Foundation, an NRF grant funded by the Korea Government (MSIP) (2019R1A2C2085302) and KMPC (2015R1D1A1AO1057610).

Institutional Review Board Statement: All animal experiments were performed following the guidelines provided by the Institutional Animal Care and Use Committee of Keimyung University (KM-2020-12R1).

Data Availability Statement: Please contact to the corresponding author for analyzed data.

Acknowledgments: We heartly acknowledge Prof. Timothy F. Osborne for kindly providing LRH-$1^{f/f}$ mice.

Conflicts of Interest: The authors declare no conflict of interest. The funders had no role in the design of the study; in the collection, analyses, or interpretation of data; in the writing of the manuscript, or in the decision to publish the results.

References

1. Fayard, E.; Auwerx, J.; Schoonjans, K. LRH-1: an orphan nuclear receptor involved in development, metabolism and steroidogenesis. *Trends Cell Biol* **2004**, *14*, 250-260, doi:10.1016/j.tcb.2004.03.008.
2. Stein, S.; Lemos, V.; Xu, P.; Demagny, H.; Wang, X.; Ryu, D.; Jimenez, V.; Bosch, F.; Luscher, T.F.; Oosterveer, M.H., et al. Impaired SUMOylation of nuclear receptor LRH-1 promotes nonalcoholic fatty liver disease. *J Clin Invest* **2017**, *127*, 583-592, doi:10.1172/JCI85499.
3. Schwaderer, J.; Phan, T.S.; Glockner, A.; Delp, J.; Leist, M.; Brunner, T.; Delgado, M.E. Pharmacological LRH-1/Nr5a2 inhibition limits pro-inflammatory cytokine production in macrophages and associated experimental hepatitis. *Cell Death Dis* **2020**, *11*, 154, doi:10.1038/s41419-020-2348-9.
4. Holmstrom, S.R.; Deering, T.; Swift, G.H.; Poelwijk, F.J.; Mangelsdorf, D.J.; Kliewer, S.A.; MacDonald, R.J. LRH-1 and PTF1-L coregulate an exocrine pancreas-specific transcriptional network for digestive function. *Genes Dev* **2011**, *25*, 1674-1679, doi:10.1101/gad.16860911.
5. Duggavathi, R.; Volle, D.H.; Mataki, C.; Antal, M.C.; Messaddeq, N.; Auwerx, J.; Murphy, B.D.; Schoonjans, K. Liver receptor homolog 1 is essential for ovulation. *Genes Dev* **2008**, *22*, 1871-1876, doi:10.1101/gad.472008.
6. Mueller, M.; Cima, I.; Noti, M.; Fuhrer, A.; Jakob, S.; Dubuquoy, L.; Schoonjans, K.; Brunner, T. The nuclear receptor LRH-1 critically regulates extra-adrenal glucocorticoid synthesis in the intestine. *J Exp Med* **2006**, *203*, 2057-2062, doi:10.1084/jem.20060357.
7. Choi, S.; Dong, B.; Lin, C.J.; Heo, M.J.; Kim, K.H.; Sun, Z.; Wagner, M.; Putluri, N.; Suh, J.M.; Wang, M.C., et al. Methyl-sensing nuclear receptor liver receptor homolog-1 regulates mitochondrial function in mouse hepatocytes. *Hepatology* **2020**, *71*, 1055-1069, doi:10.1002/hep.30884.
8. Miranda, D.A.; Krause, W.C.; Cazenave-Gassiot, A.; Suzawa, M.; Escusa, H.; Foo, J.C.; Shihadih, D.S.; Stahl, A.; Fitch, M.; Nyangau, E., et al. LRH-1 regulates hepatic lipid homeostasis and maintains arachidonoyl phospholipid pools critical for phospholipid diversity. *JCI Insight* **2018**, *3*, e96151, doi:10.1172/jci.insight.96151.
9. Mamrosh, J.L.; Lee, J.M.; Wagner, M.; Stambrook, P.J.; Whitby, R.J.; Sifers, R.N.; Wu, S.P.; Tsai, M.J.; Demayo, F.J.; Moore, D.D. Nuclear receptor LRH-1/NR5A2 is required and targetable for liver endoplasmic reticulum stress resolution. *Elife* **2014**, *3*, e01694, doi:10.7554/eLife.01694.
10. Keenan, S.N.; Meex, R.C.; Lo, J.C.Y.; Ryan, A.; Nie, S.; Montgomery, M.K.; Watt, M.J. Perilipin 5 Deletion in Hepatocytes Remodels Lipid Metabolism and Causes Hepatic Insulin Resistance in Mice. *Diabetes* **2019**, *68*, 543-555, doi:10.2337/db18-0670.
11. Kimmel, A.R.; Sztalryd, C. Perilipin 5, a lipid droplet protein adapted to mitochondrial energy utilization. *Curr Opin Lipidol* **2014**, *25*, 110-117, doi:10.1097/MOL.0000000000000057.
12. Khor, V.K.; Shen, W.J.; Kraemer, F.B. Lipid droplet metabolism. *Curr Opin Clin Nutr Metab Care* **2013**, *16*, 632-637, doi:10.1097/MCO.0b013e3283651106.
13. Pol, A.; Gross, S.P.; Parton, R.G. Review: biogenesis of the multifunctional lipid droplet: lipids, proteins, and sites. *J Cell Biol* **2014**, *204*, 635-646, doi:10.1083/jcb.201311051.
14. Langhi, C.; Marquart, T.J.; Allen, R.M.; Baldan, A. Perilipin-5 is regulated by statins and controls triglyceride contents in the hepatocyte. *J Hepatol* **2014**, *61*, 358-365, doi:10.1016/j.jhep.2014.04.009.
15. Tan, Y.; Jin, Y.; Wang, Q.; Huang, J.; Wu, X.; Ren, Z. Perilipin 5 protects against cellular oxidative stress by enhancing mitochondrial function in HepG2 cells. *Cells* **2019**, *8*, doi:10.3390/cells8101241.
16. Yokota, S.; Nakamura, K.; Ando, M.; Kamei, H.; Hakuno, F.; Takahashi, S.; Shibata, S. Acetylcholinesterase (AChE) inhibition aggravates fasting-induced triglyceride accumulation in the mouse liver. *FEBS Open Bio* **2014**, *4*, 905-914, doi:10.1016/j.fob.2014.10.009.

17. Li, Y.; Chao, X.; Yang, L.; Lu, Q.; Li, T.; Ding, W.X.; Ni, H.M. Impaired fasting-induced adaptive lipid droplet biogenesis in liver-specific Atg5-deficient mouse liver is mediated by persistent nuclear factor-like 2 activation. *Am J Pathol* **2018**, *188*, 1833-1846, doi:10.1016/j.ajpath.2018.04.015.
18. Geisler, C.E.; Hepler, C.; Higgins, M.R.; Renquist, B.J. Hepatic adaptations to maintain metabolic homeostasis in response to fasting and refeeding in mice. *Nutr Metab (Lond)* **2016**, *13*, 62, doi:10.1186/s12986-016-0122-x.
19. Asimakopoulou, A.; Engel, K.M.; Gassler, N.; Bracht, T.; Sitek, B.; Buhl, E.M.; Kalampoka, S.; Pinoe-Schmidt, M.; van Helden, J.; Schiller, J., et al. Deletion of perilipin 5 protects against hepatic injury in nonalcoholic fatty liver disease via missing inflammasome activation. *Cells* **2020**, *9*, doi:10.3390/cells9061346.
20. Gallardo-Montejano, V.I.; Saxena, G.; Kusminski, C.M.; Yang, C.; McAfee, J.L.; Hahner, L.; Hoch, K.; Dubinsky, W.; Narkar, V.A.; Bickel, P.E. Nuclear Perilipin 5 integrates lipid droplet lipolysis with PGC-1alpha/SIRT1-dependent transcriptional regulation of mitochondrial function. *Nat Commun* **2016**, *7*, 12723, doi:10.1038/ncomms12723.
21. Lee, J.H.; Go, Y.; Kim, D.Y.; Lee, S.H.; Kim, O.H.; Jeon, Y.H.; Kwon, T.K.; Bae, J.H.; Song, D.K.; Rhyu, I.J., et al. Isocitrate dehydrogenase 2 protects mice from high-fat diet-induced metabolic stress by limiting oxidative damage to the mitochondria from brown adipose tissue. *Exp Mol Med* **2020**, *52*, 238-252, doi:10.1038/s12276-020-0379-z.
22. Lee, J.S.; Bae, S.; Kang, H.S.; Im, S.S.; Moon, Y.A. Liver receptor homolog-1 regulates mouse superoxide dismutase 2. *Biochem Biophys Res Commun* **2017**, *489*, 299-304, doi:10.1016/j.bbrc.2017.05.144.
23. Im, S.S.; Hammond, L.E.; Yousef, L.; Nugas-Selby, C.; Shin, D.J.; Seo, Y.K.; Fong, L.G.; Young, S.G.; Osborne, T.F. Sterol regulatory element binding protein 1a regulates hepatic fatty acid partitioning by activating acetyl coenzyme A carboxylase 2. *Mol Cell Biol* **2009**, *29*, 4864-4872, doi:10.1128/MCB.00553-09.
24. Du, J.; Hou, J.; Feng, J.; Zhou, H.; Zhao, H.; Yang, D.; Li; Yang, Y.; Pei, H. Plin5/p-Plin5 guards diabetic CMECs by regulating FFAs metabolism bidirectionally. *Oxid Med Cell Longev* **2019**, *2019*, 8690746, doi:10.1155/2019/8690746.
25. Weber, M.; Mera, P.; Casas, J.; Salvador, J.; Rodriguez, A.; Alonso, S.; Sebastian, D.; Soler-Vazquez, M.C.; Montironi, C.; Recalde, S., et al. Liver CPT1A gene therapy reduces diet-induced hepatic steatosis in mice and highlights potential lipid biomarkers for human NAFLD. *FASEB J* **2020**, 10.1096/fj.202000678R, doi:10.1096/fj.202000678R.
26. Lin, X.; Liu, Y.B.; Hu, H. Metabolic role of fibroblast growth factor 21 in liver, adipose and nervous system tissues. *Biomed Rep* **2017**, *6*, 495-502, doi:10.3892/br.2017.890.
27. Chong, H.K.; Biesinger, J.; Seo, Y.K.; Xie, X.; Osborne, T.F. Genome-wide analysis of hepatic LRH-1 reveals a promoter binding preference and suggests a role in regulating genes of lipid metabolism in concert with FXR. *BMC Genomics* **2012**, *13*, 51, doi:10.1186/1471-2164-13-51.
28. Oosterveer, M.H.; Mataki, C.; Yamamoto, H.; Harach, T.; Moullan, N.; van Dijk, T.H.; Ayuso, E.; Bosch, F.; Postic, C.; Groen, A.K., et al. LRH-1-dependent glucose sensing determines intermediary metabolism in liver. *J Clin Invest* **2012**, *122*, 2817-2826, doi:10.1172/JCI62368.
29. Wang, C.; Zhao, Y.; Gao, X.; Li, L.; Yuan, Y.; Liu, F.; Zhang, L.; Wu, J.; Hu, P.; Zhang, X., et al. Perilipin 5 improves hepatic lipotoxicity by inhibiting lipolysis. *Hepatology* **2015**, *61*, 870-882, doi:10.1002/hep.27409.
30. Khalil, A.; Cevik, S.E.; Hung, S.; Kolla, S.; Roy, M.A.; Suvorov, A. Developmental Exposure to 2,2',4,4'-Tetrabromodiphenyl Ether Permanently Alters Blood-Liver Balance of Lipids in Male Mice. *Front Endocrinol (Lausanne)* **2018**, *9*, 548, doi:10.3389/fendo.2018.00548.
31. Ameen, C.; Edvardsson, U.; Ljungberg, A.; Asp, L.; Akerblad, P.; Tuneld, A.; Olofsson, S.O.; Linden, D.; Oscarsson, J. Activation of peroxisome proliferator-activated receptor alpha increases the expression and activity of microsomal triglyceride transfer protein in the liver. *J Biol Chem* **2005**, *280*, 1224-1229, doi:10.1074/jbc.M412107200.
32. Wolins, N.E.; Quaynor, B.K.; Skinner, J.R.; Tzekov, A.; Croce, M.A.; Gropler, M.C.; Varma, V.; Yao-Borengasser, A.; Rasouli, N.; Kern, P.A., et al. OXPAT/PAT-1 is a PPAR-induced lipid droplet protein that promotes fatty acid utilization. *Diabetes* **2006**, *55*, 3418-3428, doi:10.2337/db06-0399.
33. Seitz, C.; Huang, J.; Geiselhoringer, A.L.; Galbani-Bianchi, P.; Michalek, S.; Phan, T.S.; Reinhold, C.; Dietrich, L.; Schmidt, C.; Corazza, N., et al. The orphan nuclear receptor LRH-1/NR5a2 critically regulates T cell functions. *Sci Adv* **2019**, *5*, eaav9732, doi:10.1126/sciadv.aav9732.
34. Lee, J.M.; Lee, Y.K.; Mamrosh, J.L.; Busby, S.A.; Griffin, P.R.; Pathak, M.C.; Ortlund, E.A.; Moore, D.D. A nuclear-receptor-dependent phosphatidylcholine pathway with antidiabetic effects. *Nature* **2011**, *474*, 506-510, doi:10.1038/nature10111.
35. Mason, R.R.; Watt, M.J. Unraveling the roles of PLIN5: linking cell biology to physiology. *Trends Endocrinol Metab* **2015**, *26*, 144-152, doi:10.1016/j.tem.2015.01.005.
36. Harris, L.A.; Skinner, J.R.; Shew, T.M.; Pietka, T.A.; Abumrad, N.A.; Wolins, N.E. Perilipin 5-driven lipid droplet accumulation in skeletal muscle stimulates the expression of fibroblast growth factor 21. *Diabetes* **2015**, *64*, 2757-2768, doi:10.2337/db14-1035.